

Simulated and Observed Variations in Atmospheric CO₂ Over a Wisconsin Forest

A. Scott Denning^{*}, Melville Nicholls^{*}, Lara Prihodko^{*}, Ian Baker^{*}, Pier-Luigi Vidale[†], Kenneth Davis^{††}, and Peter Bakwin[‡]

^{*}Department of Atmospheric Science, Colorado State University, Fort Collins, CO 80523-1371, USA, [†]Natural Resource Ecology Laboratory, Colorado State University, Fort Collins, CO 80523, USA, [†]Climate Research ETH, Zürich, Switzerland, ^{††}Department of Meteorology, The Pennsylvania State University, University Park, PA 16802-5013, USA, [‡]Climate Monitoring and Diagnostics Laboratory, NOAA/OAR, R/CMDL1, Boulder, CO 80303

Abstract

Ecosystem fluxes of energy, water, and CO₂ result in spatial and temporal variations in atmospheric properties. In principal, these variations can be used to quantify the fluxes through inverse modeling of atmospheric transport, and can improve understanding of processes and falsifiability of models. We investigated the influence of ecosystem fluxes on atmospheric CO₂ in the vicinity of the WLEF-TV tower in Wisconsin using an ecophysiological model (SiB2) coupled to an atmospheric model (RAMS). Model parameters were specified from satellite imagery and soil texture data (Prihodko et al, this issue). In a companion paper (Baker et al, this issue), fluxes in the immediate tower vicinity have been compared to eddy covariance fluxes measured at the tower, with meteorology specified from tower sensors. Results were encouraging with respect to the ability of the model to capture observed diurnal cycles of fluxes. Here, the effects of fluxes in the tower footprint were also investigated by coupling SiB2 to a high-resolution atmospheric simulation, so that the model physiology could affect the meteorological environment. These experiments were successful in reproducing observed fluxes and concentration gradients during the day and at night, but revealed problems during transitions at sunrise and sunset that appear to be related to the canopy radiation parameterization in SiB2.

Keywords: net ecosystem exchange, atmosphere-biosphere interactions, large eddy simulation, mesoscale modeling

Correspondence: A. Scott Denning, fax: +1-970-491-6936, email: denning@atmos.colostate.edu

Introduction

The global carbon budget has been studied in terms of both local measurements and modeling of the processes involved, and in terms of the effects of these processes at hemispheric and global scale. The process-based studies are crucial to understanding and hopefully predicting changes in the Earth system that control the concentration of atmospheric CO₂, but the representativeness of any given field study is difficult or impossible to assess. The challenge to process-oriented researchers is to extrapolate their results to regional, continental, and global scales, from the “bottom up.” Conversely, global inverse calculations of the carbon budget have the advantage of providing quantitative information about the integrated effects of physical, biogeochemical, and anthropogenic processes over huge spatial areas. These “top down” studies provide a spatially-integrated “snapshot” of the current state of the carbon cycle, but can provide little information about the processes responsible or how these might change in the future. Inverse methods are able to provide robust estimates of fluxes only at the largest spatial scales: global and hemispheric annual means are well constrained, but different transport models or inverse methods produce very different estimates of even continental fluxes on monthly basis (e.g., Fan et al, 1998; Rayner et al, 1999; Gurney et al, 2001). The challenge to inverse modelers is to refine the resolution of their calculations to the point that they can provide a meaningful integral constraint for the “bottom-up” studies of processes.

Very few studies have addressed the gap in spatial scales between whole-ecosystem studies of long-term carbon flux by eddy covariance (with a “footprint” of perhaps 1 km²) and time-dependent tracer transport inversions (which are difficult to interpret over areas much smaller than 10⁸ km²). This huge spatial gap was identified as a priority for future

data collection in a recent set of recommendations for carbon cycle research (Sarmiento et al, 1999), but the design of mesoscale observing systems will require preliminary studies of the variability of CO₂ and other relevant tracers to be effective.

Mesoscale studies of atmosphere-biosphere exchanges of heat, water, momentum, and CO₂ can also provide an opportunity to test process-based models in new ways. Ecophysiological models have long been tested against point measurements at tower sites, but the spatial scaling of these processes to larger regions is difficult to test. The data record collected over six years at the WLEF-TV tower in Wisconsin provides an opportunity to test such scaling in land-atmosphere models, because of its ability to sample above the immediate surface layer environment of the forest below (Bakwin et al, 1999). The flux footprint of the tower expands with height and the concentration record at the top of the tower reflects upwind fluxes for hundreds of km.

The atmospheric model employed in this study is applicable to a wide range of spatial scales, from the mesoscale down to the small scale turbulent eddies occurring in the atmospheric boundary layer. Here we test the coupled ecophysiological-atmospheric modeling system, by running it in two-dimensional mode and comparing results of a high resolution simulation with observations made for a two-day period, at the WLEF-TV tower. Canopy and soil parameters for the ecophysiology model are specified from satellite imagery and a database of soil textural properties (Prihodko et al., this issue).

The ecophysiology model was tested at the scale of the immediate flux footprint for three years (1997-1999), and found to be reasonably successful in capturing fluxes of heat, moisture, and CO₂ over diurnal and synoptic time scales (Baker et al., this issue). This paper presents first results from experiments with a coupled mesoscale model of forest-atmosphere interactions in the vicinity of the WLEF tower.

Methods

The WLEF-TV Tower Site

The Wisconsin forest site is the location of a 450 meter tall television transmission tower (WLEF-TV, 45° 55' N, 90° 10' W), located in the Chequamegon National Forest, 24 km west of Park Falls, WI. The region is in a heavily forested zone of low relief. The region immediately surrounding the tower is dominated by boreal lowland and wetland forests typical of the region. Much of the area was logged, mainly for pine, during 1860-1920, and has since regrown. The concentration of CO₂ has been measured continuously at 6 heights (11, 30, 76, 122, 244, and 396 m above the ground) since October, 1994, and CO₂ flux has been measured at three heights at this tower (30, 122 and 396 m) since 1996. Micrometeorology and soil temperature and moisture data are collected at the site or at the nearby USDA Forest Sciences Laboratory. Another significant advantage of this site is that the great height of the tower provides the opportunity for observing the carbon balance over a “footprint” that increases with height on the tower up to several km² for the highest observing platform, which is approximately two orders of magnitude greater than other Ameriflux monitoring sites.

Model Descriptions

The Simple Biosphere (SiB) Model, developed by Sellers et al. (1986), has undergone substantial modification (Sellers et al., 1996a, b), and is now referred to as SiB2. The number of biome-specific parameters has been reduced, and most are now derived directly from processed satellite data rather than prescribed from the literature. The vegetation canopy has been reduced to a single layer. Another major change is in the parameterization of stomatal and canopy conductance used in the calculation of the surface energy budget over land. This parameterization involves the direct calculation of

the rate of carbon assimilation by photosynthesis, making possible the calculation of CO₂ exchange between the global atmosphere and the terrestrial biota on a timestep of several minutes (Denning et al., 1996a,b; Zhang et al., 1996). Photosynthetic carbon assimilation is linked to stomatal conductance and thence to the surface energy budget and atmospheric climate by the Ball-Berry equation (Ball, 1988; Collatz et al., 1991, 1992; Sellers et al., 1992, 1996a).

Model parameters for SiB2 were specified from AVHRR imagery and soil texture data (Prihodko et al., this issue). Simulated variations in fluxes of energy, water, and carbon using SiB2 driven by observed meteorology for the site have been compared to observations by Baker et al. (this issue). Multiyear simulations driven by site meteorology were used to specify initial conditions (e.g., soil moisture and temperature) for SiB2 in the simulations described below.

The Regional Atmospheric Modeling System (RAMS) was developed at Colorado State University in order to facilitate research of predominantly mesoscale and cloud-scale phenomena (Pielke, 1974; Tripoli and Cotton, 1982; Pielke et al., 1992; Nicholls et al., 1995). A significant feature of the model is the incorporation of a telescoping nested-grid capability, which enables the simulation of phenomena involving a wide range of spatial scales. The model has been applied to the simulation of flows at scales as small as buildings (Nicholls et al., 1993; Nicholls et al., 1995; Pielke and Nicholls, 1996) and so is aptly suited for studying the interactions between the atmosphere and terrestrial ecosystems which take place at many spatial scales. RAMS is a non-hydrostatic model and contains time-dependent equations for velocity, non-dimensional pressure perturbation, ice-liquid water potential temperature (see Tripoli and Cotton, 1981), total water mixing ratio, and cloud microphysics. Vapor mixing ratio and potential

temperature are diagnostic. The model is compressible permitting the propagation of sound waves. For computational efficiency a time-splitting procedure is employed, whereby the terms responsible for high frequency acoustic waves are solved with a small time step and low frequency terms with a long time step (Klemp and Wilhelmson, 1978; Cotton and Tripoli, 1978; Nicholls and Pielke, 2000). Velocity components and pressure are updated using leapfrog differencing and all other variables are advanced using forward differencing on the long time step. A forward-backward scheme is used on the small time step. A second-order-in-space advection scheme is employed. The turbulence closure scheme of Deardorff (1980) is used in this study which employs a prognostic sub-grid turbulent kinetic energy. The two-stream radiation scheme developed by Harrington (1997) is used. At the lower boundary the surface fluxes in this study are computed by the coupled SiB2 model (discussed later). The cyclic lateral boundaries option is used at the upper levels of the domain the Rayleigh friction option is applied to reduce artificial reflection of gravity waves from the rigid lid.

The lowest level above the surface in the RAMS model is the reference level at which atmospheric boundary layer values of temperature, vapor pressure, wind velocity and carbon dioxide partial pressure are provided as upper boundary conditions to SiB2. Additionally, the direct and diffuse components of short wave and near infrared radiation incident at the surface are provided from the RAMS radiation scheme. The surface layer, which is between the surface and the reference level is incorporated as part of the SiB2 model and is based on the scheme of Holtslag and Boville (1993). The input variables provided by RAMS to SiB2 are updated every minute of simulation time. SiB2 provides back to RAMS, at the reference level, fluxes of heat, moisture, momentum and carbon dioxide, as well as the upwelling radiation.

To investigate detailed processes in the immediate vicinity of the tower, we performed a high resolution two-dimensional simulation of the 26th and 27th of July, 1997. The SiB2 parameters derived at the WLEF site (the central pixel in the parameter fields derived by Pridhoko et al (this issue)) were used, without any tuning to the specific field site. Horizontally homogeneous vertical profiles of temperature, moisture and wind were specified which were obtained from the isentropic analysis made for the variable initialization run (described below) at 6 a.m. on the 26th. A horizontal grid increment of 100 m was used and the vertical grid increment at the surface was 20 m, which was gradually stretched with height to the top of the domain. The domain width was 8 km and the height was 7 km, roughly the extent of the flux footprint at the top of the tower in moderately turbulent conditions. Simulations were carried out both with and without the cloud microphysics scheme activated. The RAMS microphysics scheme (Walko et al., 1995) includes both the liquid and ice phases of water substance. For the period of this study, the clouds were most likely scattered shallow cumulus composed of liquid water. The microphysics scheme has two categories of liquid water: (1) cloud water droplets which advect with air parcels, and (2) rain water droplets which are larger and are allowed to fall relative to air parcels. The cloud water droplets are mono-dispersed and the cloud condensation nuclei was set to $1,000 \text{ cm}^{-3}$, typical of continental air masses. A Marshall-Palmer distribution was employed for rain water droplets with a mean mass diameter of 1 mm. For the shallow cumulus clouds simulated in this study, most of the liquid water content remained in the cloud water category. The purpose of these simulations was to provide a realistic simulation of the small-scale structure and processes occurring at the WLEF site. Of course, since the domain was periodic it did not include large-scale advective influences.

Results and Discussion

Although we chose to simulate a relatively simple case with minimal cloud cover and no precipitation, occasional shallow cumulus clouds were present during the experiment. Solar radiation input to the forest varied with the passing of these clouds (Fig. 1). The simulation with clouds is not intended to reproduce the detailed occurrence of these variations, but rather to introduce a realistic degree of variance in radiative forcing to the forest ecosystem. The simulation with active cloud microphysics represented both the mean diurnal cycle of insolation and its variance better than the cloud-free simulation.

Observed sensible heat flux (from eddy covariance measurements at the tower) are compared to the high-resolution 2-D simulations in Figure 2. The model tends to overestimate the magnitude of the sensible heat flux relative to the observations, especially in the cloud-free case, during both day and night. Baker et al. (this issue) found that this discrepancy may result in part from underestimation in the analysis of the eddy flux data, based on the climatology of energy budget closure problems. Hour-to-hour variability in sensible heat flux is reasonably well-captured in the simulation with clouds. Both simulations exhibited stronger latent heat flux than observed (Fig. 3), and even the simulation with clouds underestimated the observed variability. The sum of sensible and latent heat flux simulated by the model exceeded the observed sum by almost 100 W m^{-2} at mid-day. Given that the total incoming solar radiation was approximately correct, this “extra” energy is likely due to a combination of underestimation of both albedo and soil thermal conductivity in the model (Baker et al., this issue).

Net CO_2 flux to the atmosphere was reasonably well-simulated (Fig. 4). The observations were characterized by very weak fluxes at night, followed by a “flush” of stored CO_2 as the stable layer broke up in the early morning. This phenomenon was also

simulated by the model, though nighttime respiration fluxes were stronger in the model than in the observations. This may reflect underestimation by the eddy covariance system under stable nocturnal conditions. Net uptake at mid-day was well-simulated, though the cloud-free simulation included the development of physiological stress in the middle of the second day, reducing net uptake by about 30%. Stomatal closure was much less pronounced in the simulation with clouds, because the overall radiation load was less intense, limiting canopy temperature and vapor pressure deficit.

Atmospheric CO₂ concentrations resulting from the fluxes discussed above exhibited a strong diurnal cycle (Fig. 5). The figure shows “snapshots” of CO₂ during the second day of the cloud-free simulation. Just after sunrise (7 AM, Fig. 5a), a layer of very high-concentration air was trapped under the strong inversion, which was about 200 m deep. The air just above this stable layer exhibited much lower concentrations, with a CO₂ minimum at about 600 m above the forest. The relatively lower concentrations up to about 1.5 km altitude result from uptake during the previous day. This “residual layer” of lower CO₂ is decoupled from the surface during the night because of the development of the stable layer near the surface, and would be subject to large-scale advection in the real world. The lateral boundaries for the model were periodic, however, so this residual layer has nowhere to go. By 9 AM (Fig. 5b), the turbulent boundary layer had begun to grow into the residual layer, and photosynthesis was well underway. Entrainment of air into this growing PBL diluted the high-CO₂ air left over from the nocturnal stable layer. At the same time, photosynthesis was removing CO₂ from the still-shallow PBL, producing some of the lowest concentration values seen in the experiment. By 1 PM (Fig. 5c), the depth of the convective PBL had grown to about 1500 m, with relatively well-mixed CO₂ concentration. Gradients of 1-2 ppm resulted from convective updrafts rising from the

forest with lower-than-average concentration and from downdrafts carrying above-average concentration air from the entrainment zone at the top of the PBL. Mid-day vertical gradients were extremely weak relative to the horizontal variability created by the large turbulent eddies. At 8 PM (Fig. 5d), a new stable layer had formed at the surface, but canopy activity continued, resulting in the lowest CO₂ concentrations of the entire simulation. The air above this low-CO₂ stable layer was decoupled from the surface due to the formation of the stable surface layer.

Qualitatively, the diurnal and vertical variations of the observed CO₂ concentration (Fig. 6a) shows the same pattern as the simulation. The vertical gradient built up at night in the stable layer, with concentration differences of 80 ppm between the bottom and top of the tower developing by sunrise. As the turbulence began building in the morning, this high-concentration air was diluted by entrainment from the residual layer, yet the growth of this layer led to a maximum concentration at 122 m about 2 hours after the maximum at 30 m, and an hour later at 396 m. At mid-morning, the depth of the turbulence exceeded the top of the tower, and concentrations remained well-mixed for the rest of the day. Mid-day vertical gradients were weak, with about 2 ppm lower concentrations at the base than the top of the tower. After sunset, with the cessation of photosynthesis roughly coinciding with the development of the stable layer, concentration gradients began to grow again, from the bottom up.

Maximum early-morning concentrations at the 30-m level in the cloud-free simulation (Fig. 6b) weren't as great as those in the simulation with clouds (Fig. 6c), especially on the night of the 27th. The most significant difference between the simulations and the observations, however, was in the concentrations just above the forest at sunrise and sunset. Whereas the observations showed a smooth morning transition

from high nocturnal values to the well-mixed conditions of mid-day, the simulations featured a morning concentration minimum at the lowest tower level which lasted for about two hours after sunrise. Similarly, the simulations showed an evening minimum near sunset that was not observed.

Analysis of the evening transition (Fig. 7) revealed the mechanism behind the unobserved dip in concentration that occurred in the simulations. Latent heat flux (Fig. 7a) was consistently overestimated by the model, and persisted about an hour after canopy activity was observed to cease. Sensible heat flux (Fig. 7b) became negative at about 4:30 PM in the model when the simulated latent heat flux exceeded the net radiation, forming a very shallow stable layer near the surface. A very weak stable layer was in fact observed for this day, but it formed about an hour later than in the model, and remained much less stable than the model until about 9 PM. Simulated CO₂ flux was also stronger than observed throughout the late afternoon, and the negative net ecosystem exchange continued until 7 PM (Fig. 7c). Actual NEE was observed to decrease gradually from about 1 PM and reach zero about 6 PM. From about 4:30 until 7 PM, the model ecosystem was drawing CO₂ out of a very shallow stable layer which prevented replenishment of CO₂ from the air aloft. The persistence of nearly mid-day levels of canopy activity (photosynthesis and transpiration) into the late afternoon is consistent with the multiyear offline simulations reported by Baker et al. (this issue), and probably results from overestimation of canopy-averaged light-use efficiency in SiB. This caused the simulated CO₂ concentration (Fig. 7d) to decrease sharply just before sunset, reaching a minimum of 340 ppm, whereas the observed concentration was essentially constant through the period until it began to rise with the nearly simultaneous onset of positive NEE and negative sensible heat flux.

Conclusions

The coupled SiB2-RAMS model was reasonably successful in representing observed diurnal variations in fluxes of radiation, heat, water, and CO₂ at the WLEF tower site. Advantages of the coupled model relative to the offline simulations reported by Baker et al. (this issue) include the representation of the feedbacks between surface fluxes and PBL properties and the ability to compare simulated atmospheric CO₂ concentration to observations as an additional criterion for model evaluation. The diurnal cycle of the evolution of the PBL and the vertical profile of CO₂ in the high-resolution 2D simulations is fairly consistent with the tower observations. The major exception is the development of a shallow CO₂ minimum in the simulations just before sunset. This arises because of a tendency of the model to overestimate late afternoon canopy activity (transpiration and photosynthesis), leading to persistent CO₂ uptake under a stable layer that forms about an hour too early. This phenomenon is attributed to misrepresentation of the extinction of direct beam radiation in SiB, resulting in overestimation of canopy-average light-use efficiency, and was also noted by Baker et al (this volume). While the deviation of the simulated fluxes from the observations was fairly subtle, the effect on simulated CO₂ concentrations was obvious. This is an important advantage of the fully coupled simulations, and shows that prediction of an atmospheric scalar (CO₂) can in fact reveal subtle problems with the treatment of canopy biophysics.

Acknowledgements

This research was funded in part by the South-Central Regional Center (SCRC) of the National Institute for Global Environmental Change (NIGEC) through the U.S. Department of Energy (Cooperative Agreement No. DE-FC03-90ER61010, Contract No. TUL-106-00/01). Any opinions, findings and conclusions or recommendations expressed herein are those of the authors and do not necessarily reflect the view of the DOE. Support was also provided by COBRA (Contract No. ATM-982-1044), and by the

Terrestrial Ecosystems program of the US Department of Energy (Subcontract Number 1948-CSU-USDOE-3008).

References

- Ball, J. T., 1988. An analysis of stomatal conductance. Ph.D. Thesis, Stanford University, Stanford, Calif.
- Baker, I., A. S. Denning, N. Hanan, L. Prihodko, P.-L. Vidale, K. Davis, and P. Bakwin, 2001. Simulated and Observed Fluxes of Sensible and Latent Heat and CO₂ at the WLEF-TV Tower Using SiB2.5. Submitted to *Global Change Biology*.
- Berry, J. A., Sellers, P. J., Randall, D. A., Collatz, G. J., Colello, G. D., Denning, A. S., Fu, W. and Grivet, C., 1998. SiB2, a model for simulation of biological processes within a climate model. In: *Scaling Up* (Eds. P. van Gardingen, G. Moody and P. Curran), Society for Experimental Biology, Cambridge University Press, in press.
- Collatz, G. J., Ball, J. T., Grivet, C. and Berry, J. A., 1991. Physiological and environmental regulation of stomatal conductance, photosynthesis, and transpiration: a model that includes a laminar boundary layer. *Agric. and Forest Meteorol.*, **54**, 107-136.
- Collatz, G. J., Ribas-Carbo, M. and Berry, J. A., 1992. Coupled photosynthesis-stomatal conductance model for leaves of C4 plants. *Aust. J. Plant Physiol.*, **19**, 519-538.
- Conway, T. J., P. P. Tans, L. S. Waterman, K. Thoning, D. R. Kitzis, K. A. Masarie, and N. Zhang, 1994: Evidence for interannual variability of the carbon cycle from the NOAA/CMDL global air sampling network. *Jour. Geophys. Res.*, **99**, 22831-22855.
- Cotton, W. R. and G. J. Tripoli, 1978: Cumulus convection in shear flow: Three-dimensional numerical experiments. *J. Atmos. Sci.*, **35**, 1503-1521.
- Deardorff, J. W., 1980: Stratocumulus-capped mixed layers derived from a three-dimensional model. *Boundary Layer Met.*, **18**, 495-527.
- Denning, A. S., I. Y. Fung, and D. A. Randall, 1995: Latitudinal gradient of atmospheric CO₂ due to seasonal exchange with land biota. *Nature*, **376**, 240-243.
- Denning, A. S., J. G. Collatz, C. Zhang, D. A. Randall, J. A. Berry, P. J. Sellers, G. D. Colello, and D. A. Dazlich, 1996a. Simulations of terrestrial carbon metabolism and atmospheric CO₂ in a general circulation model. Part 1: Surface carbon fluxes. *Tellus*, **48B**, 521-542.
- Denning, A. S., D. A. Randall, G. J. Collatz, and P. J. Sellers, 1996b. Simulations of terrestrial carbon metabolism and atmospheric CO₂ in a general circulation model. Part 2: Spatial and temporal variations of atmospheric CO₂. *Tellus*, **48B**, 543-567.
- Enting, I. G., Trudinger, C. M. and Francey, R. J., 1995. A synthesis inversion of the concentration and delta ¹³C of atmospheric CO₂. *Tellus*, **47B**, 35-52.
- Fan, S.-M., Gloor, M., Mahlman, J., Pacala, S., Sarmiento, J., Takahashi, T. and Tans, P., 1998. A large terrestrial carbon sink in North America implied by atmospheric and oceanic carbon dioxide data and models. *Science* **282**, 442-446.

- Farquhar, G. D., von Caemmerer, S. and Berry, J. A., 1980. A biochemical model of photosynthetic CO₂ assimilation in C3 plants. *Planta*, **149**, 78-90.
- Hansen, M., DeFries, R., Townshend, J. R. G. and Sohlberg, R., 1999, Global land cover classification at 1 km resolution using a decision tree classifier, *International Journal of Remote Sensing*, in press.
- Harrington, J. Y., 1997: The effects of radiative and microphysical processes on simulated warm and transition season Arctic stratus. Ph.D. dissertation, Colorado State University, 289 pp. [Available from Colorado State University, Dept. of Atmospheric Science, Fort Collins, CO 80523.]
- Holtzlag, A. A. and B. A. Boville, 1993: Local versus nonlocal boundary-layer diffusion in a global climate model. *J. Clim.*, **6**, 1825-1842.
- Intergovernmental Panel on Climate Change (IPCC), 1995. *Climate Change 1994: Radiative Forcing of Climate Change and an Evaluation of the IPCC IS92 Emission Scenarios* (eds. J. T. Houghton, L. G. Meira Filho, J. Bruce, H. Lee, B. A. Callander, E. Haites, N. Harris and K. Maskell). Cambridge University Press, Cambridge.
- Klemp, J. B. and R. B. Wilhelmson, 1978: The simulation of three-dimensional convective storm dynamics. *J. Atmos. Sci.*, **35**, 1070-1096.
- Los, S. O., C. O. Justice, and C. J. Tucker, A global 1 by 1 degree NDVI data set for climate studies derived from the GIMMS continental NDVI, *Int. J. Remote Sens.*, **15**, 3493-3518, 1994.
- Nicholls, M. E., R. A. Pielke and R. N. Meroney, 1993: Large eddy simulation of microburst winds flowing around a building. *J. Wind Engineering and Industrial Aerodynamics*, **46847**, 229-237.
- Nicholls, M. E., R. A. Pielke, J. L. Eastman, C. A. Finley, W. A. Lyons, C. J. Tremback, R. L. Walko, and W. R. Cotton, 1995: Applications of the RAMS numerical model to dispersion over urban areas. *Wind Climate in Cities*, J.E. Cermak et al. Eds., 703-732.
- Nicholls, M. E. and R. A. Pielke, 2000: Thermally induced compression waves and gravity waves generated by convective storms. *J. Atmos. Sci.*, **57**, 3251-3271.
- Pielke, R. A., 1974: A three-dimensional numerical model of the sea breezes over south Florida. *Mon. Wea. Rev.*, **102**, 115-139.
- Pielke, R. A., W. R. Cotton, R. L. Walko, C. J. Tremback, W. A. Lyons, L. D. Grasso, M. E. Nicholls, M. D. Moran, D. A. Wesley, T. J. Lee, and J. H. Copeland, 1992. A comprehensive meteorological modeling system RAMS. *Meteor. Atmos. Phys.*, **49**, 69-91.
- Prihodko, L., A. S. Denning, N. P. Hanan, G. J. Collatz, P. S. Bakwin, and K. Davis, 1998. Simulation and sensitivity analysis of carbon and energy fluxes at the WLEF-TV Tower site in Wisconsin, presented at Fall 1998 AGU Meeting, San Francisco.
- Prihodko, L., A. S. Denning, K. Schaefer, T. Krebs, 2001. Creating Mesoscale Land Surface Datasets for Regional Modeling of the WLEF-TV Tower Site, Wisconsin. Submitted to *Global Change Biology*.
- Sellers, P. J., Y. Mintz, Y. C. Sud, and A. Dalcher, 1986: A simple biosphere model

- (SiB) for use within general circulation models. *J. Atmos. Sci.*, **43**, 505-531.
- Sellers, P. J., Heiser, M. D., and Hall, F. G., 1992. Relations between surface conductance and spectral vegetation indices at intermediate (100 m² to 15 km²) length scales. *J. Geophys. Res.*, **97**, 19033-19059.
- Sellers, P. J., D. A. Randall, G. J. Collatz, J. Berry, C. Field, D. A. Dazlich, C. Zhang, and L. Bounoua, 1996a: A Revised Land-Surface Parameterization (SiB2) for Atmospheric GCMs. Part 1: Model formulation. *J. Clim.*, **9**, 676-705.
- Sellers, P. J., S. O. Los, C. J. Tucker, C. O. Justice, D. A. Dazlich, G. J. Collatz, and D. A. Randall, 1996b: A Revised Land-Surface Parameterization (SiB2) for Atmospheric GCMs. Part 2: The generation of global fields of terrestrial biophysical parameters from satellite data. *J. Clim.*, **9**, 706-737.
- Sellers, P. J., L. Bounoua, G. J. Collatz, D. A. Randall, D. A. Dazlich, S. O. Los, J. A. Berry, I. Fung, C. J. Tucker, C. B. Field, and T. G. Jensen, 1996c. Comparison of radiative and physiological effects of doubled atmospheric CO₂ on climate. *Science*, **271**, 1402-1406.
- Tans, P. P., Fung, I. Y. and Takahashi, T., 1990. Observational constraints on the global atmospheric CO₂ budget. *Science* **247**, 1431-1438.
- Tripoli, G. J. and W. R. Cotton, 1981: The use of ice-liquid water potential temperature as a thermodynamic variable in deep atmospheric models. *Mon. Wea. Rev.*, **109**, 1094-1102.
- Tripoli, G. J. and W. R. Cotton, 1982: The Colorado State University three-dimensional cloud/mesoscale model – 1982. Part I: General theoretical framework and sensitivity experiments. *J. de Rech. Atmos.*, **16**, 185-220.
- Walko, R. L., C. J. Tremback, R. A. Pielke, and W. R. Cotton, 1995a: An interactive nesting algorithm for stretched grids and variable nesting ratios. *J. Appl. Meteor.*, **34**, 994-999.
- Walko, R. L., W. R. Cotton, J. L. Harrington, M. P. Meyers, 1995b: New RAMS cloud microphysics parameterization. Part I: The single-moment scheme. *Atmos. Res.*, **38**, 29-621.
- Zhang, C., D. A. Dazlich, D. A. Randall, P. J. Sellers, and A. S. Denning, 1996: Calculations of the global land surface energy, water, and CO₂ fluxes with an off-line version of SiB2. *Jour. Geophys. Res.*, **101**, 19061-19075.

Figure Captions

Figure 1: Simulated and observed downward solar radiation for July 26-27, 1997. Simulations used the high-resolution two-dimensional grid. Upper panel is for cloudless conditions, and the lower panel shows results including passing clouds.

Figure 2: Simulated and observed sensible heat fluxes for July 26-27, 1997, at 30 m. Upper panel is for cloudless conditions, and the lower panel shows results including passing clouds.

Figure 3: As in Figure 2, but for latent heat flux.

Figure 4: As in Figure 2, but for CO₂ flux.

Figure 5: cross-sections of simulated CO₂ concentration in the lower troposphere. Top-left panel is for 7 AM?; Top-right panel is for 9 AM?; Bottom-right panel is for 1 PM; Bottom-right panel is for 8 PM.

Figure 6: Comparison of simulated and observed CO₂ concentration at three levels on the WLEF-TV tower, with and without cloud microphysics.

Figure 7: Latent heat flux, sensible heat flux, carbon dioxide flux, and carbon dioxide concentration in late afternoon, showing the early development of the stable layer in SiB-RAMS which is not observed.

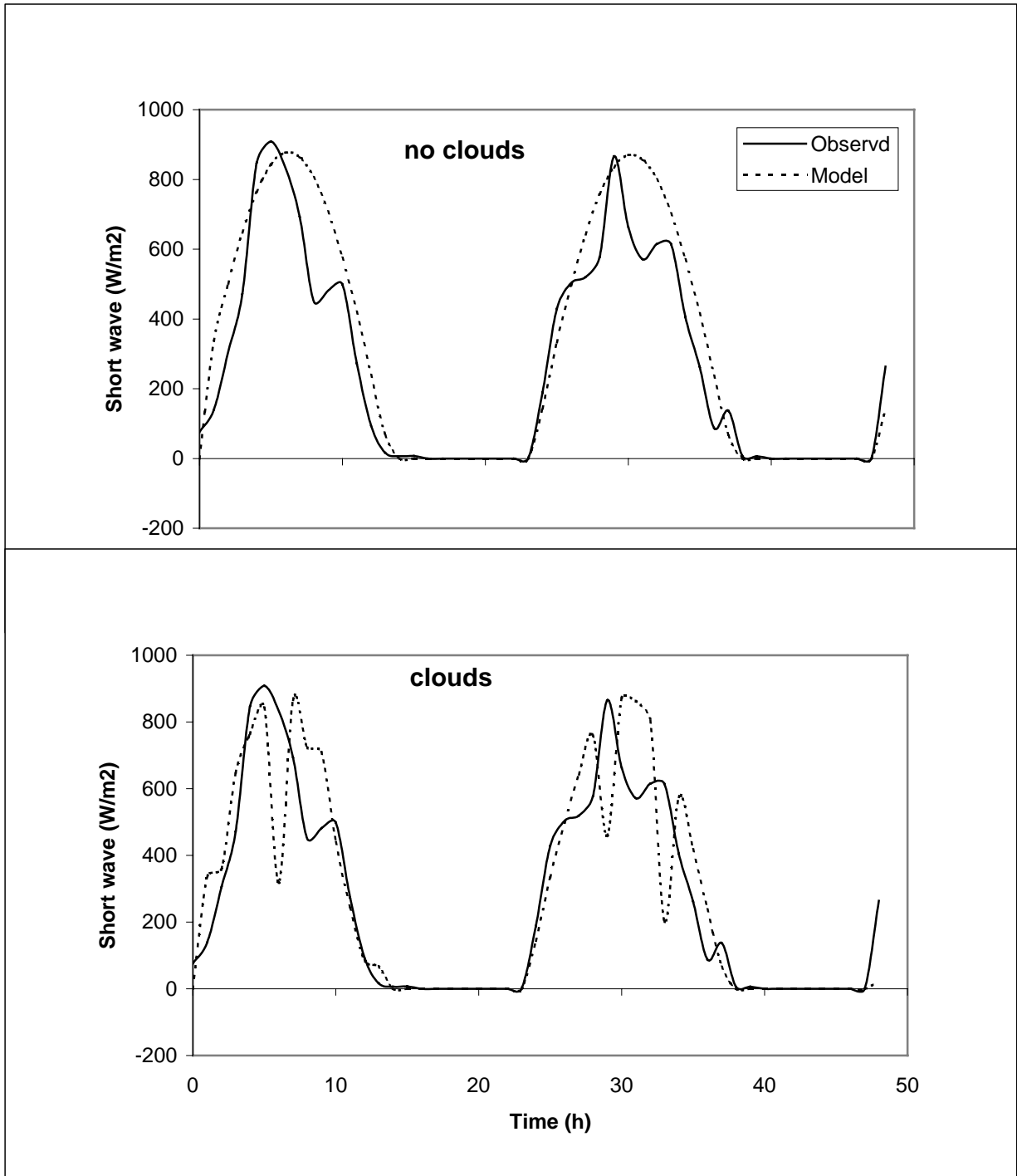


Figure 1: Simulated and observed downward solar radiation for July 26-27, 1997. Simulations used the high-resolution two-dimensional grid. Upper panel is for cloudless conditions, and the lower panel shows results including passing clouds.

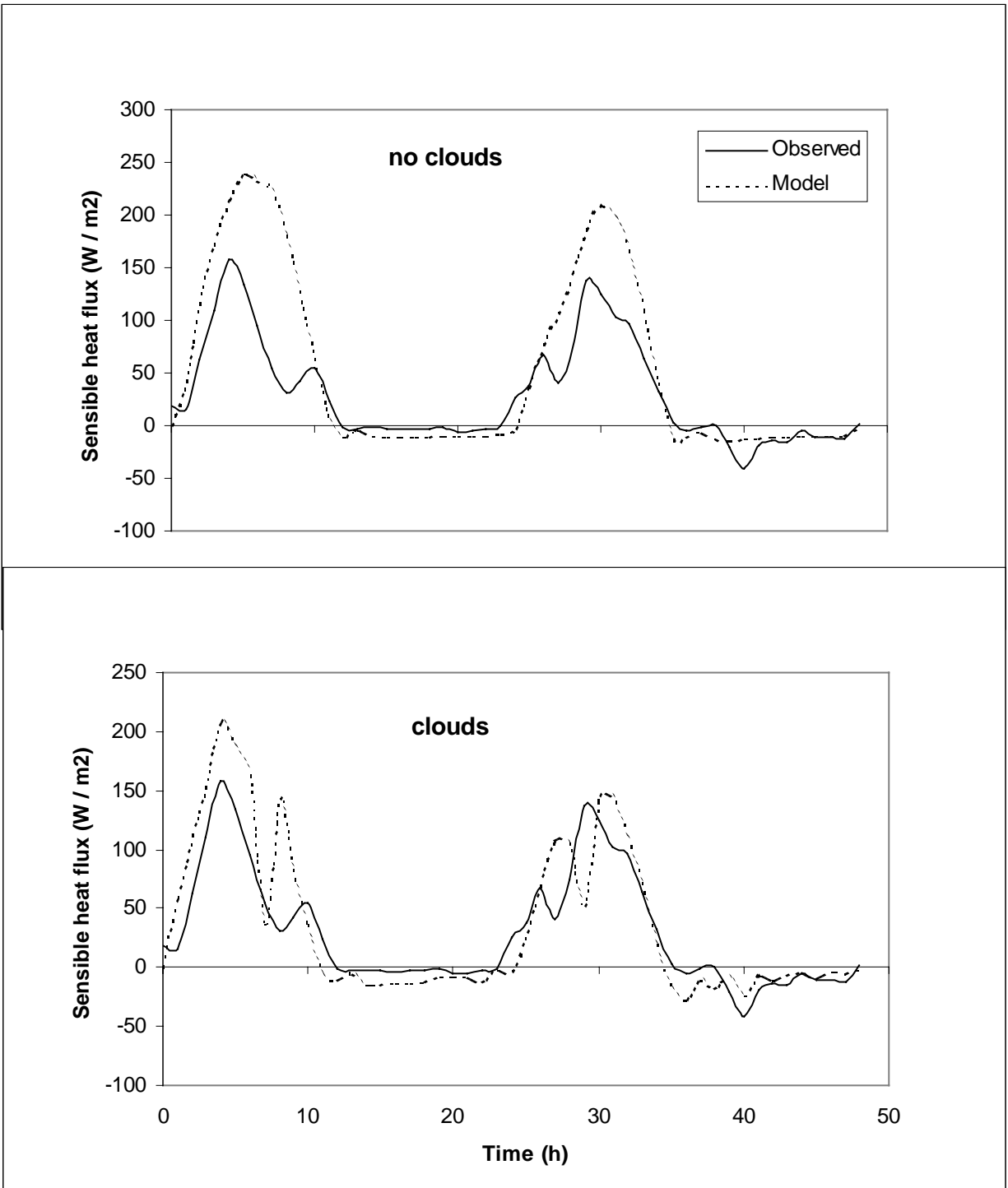
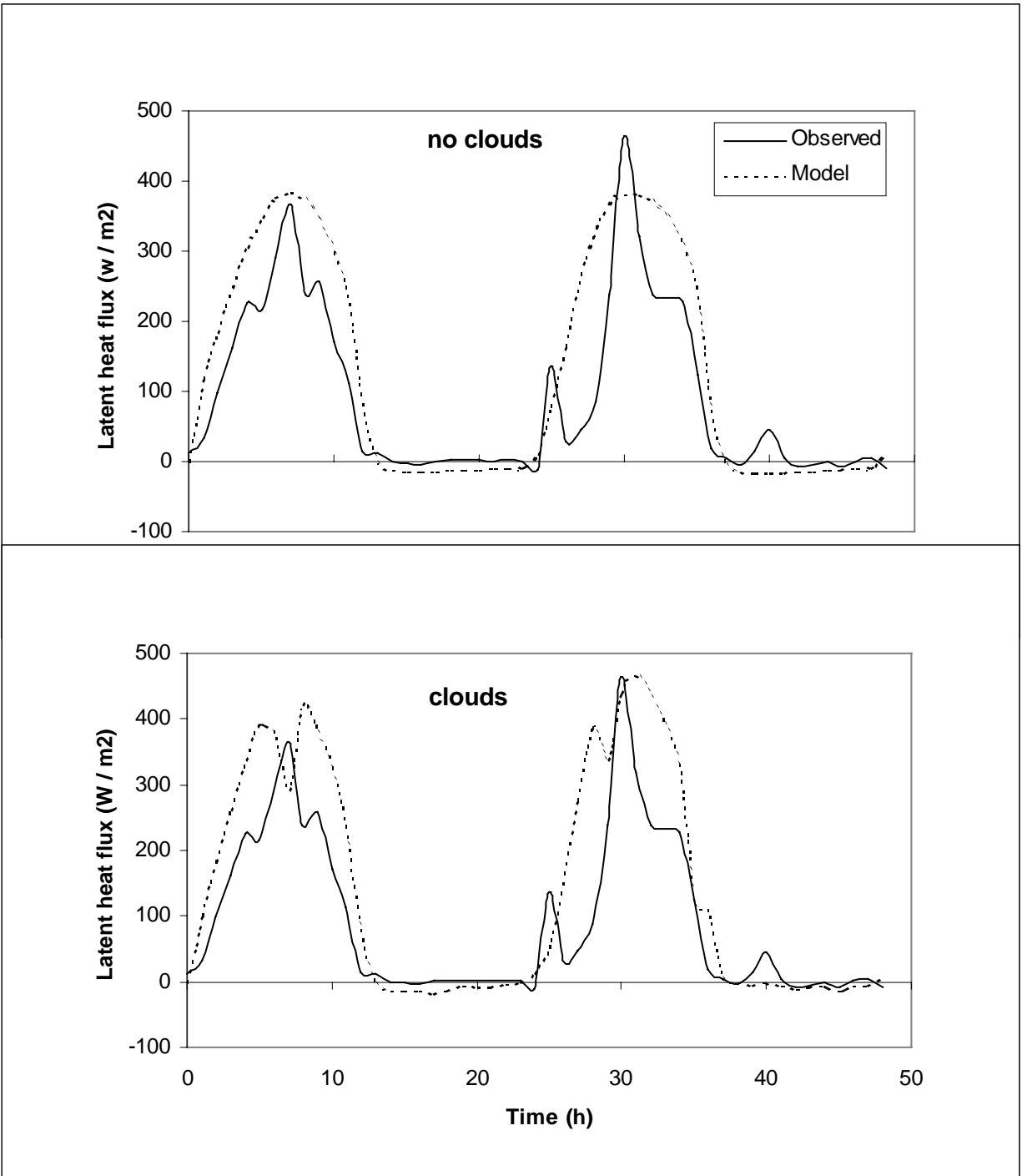


Figure 2: Simulated and observed sensible heat fluxes for July 26-27, 1997. Simulations used the high-resolution two-dimensional grid. Upper panel is for cloudless conditions, and the lower panel shows results including passing clouds. **What tower level?**

Figure 3: As for Fig 1, but for latent heat flux.



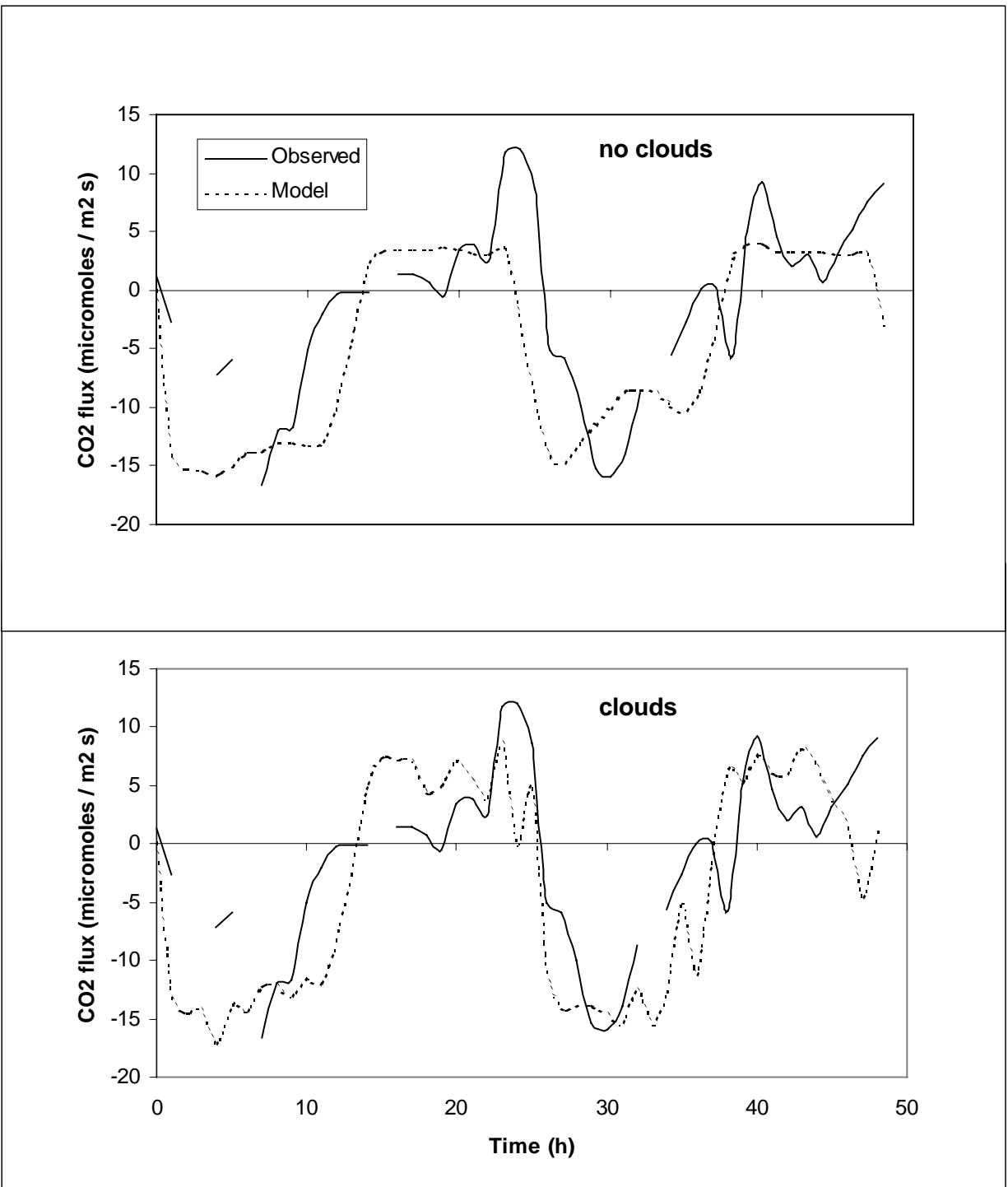


Figure 4: As in Fig 1, but for CO₂ flux at 122 m?

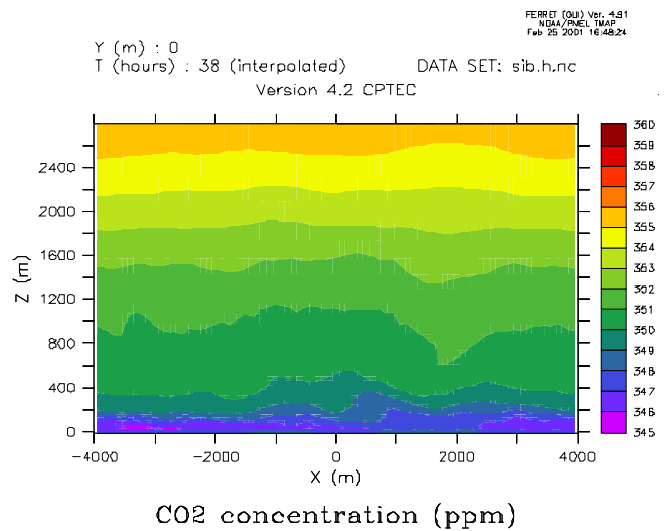
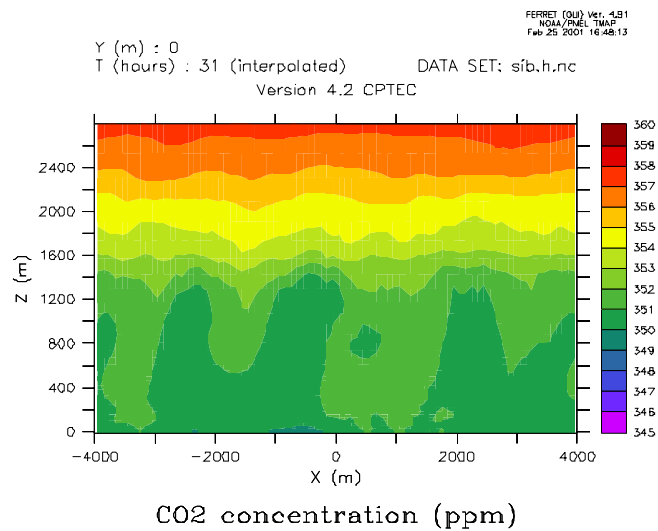
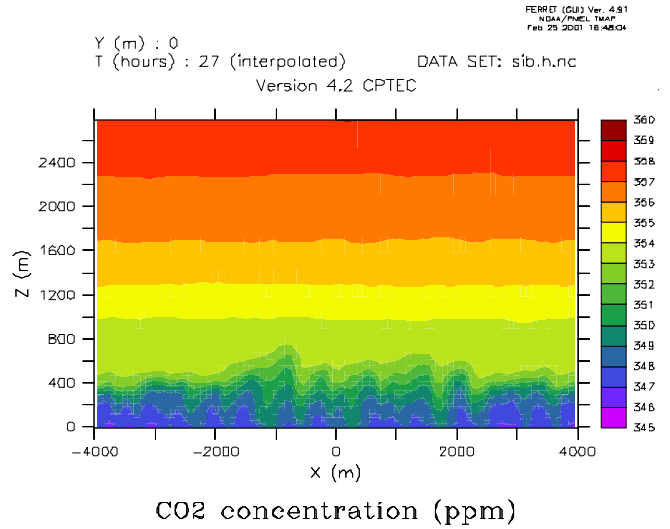
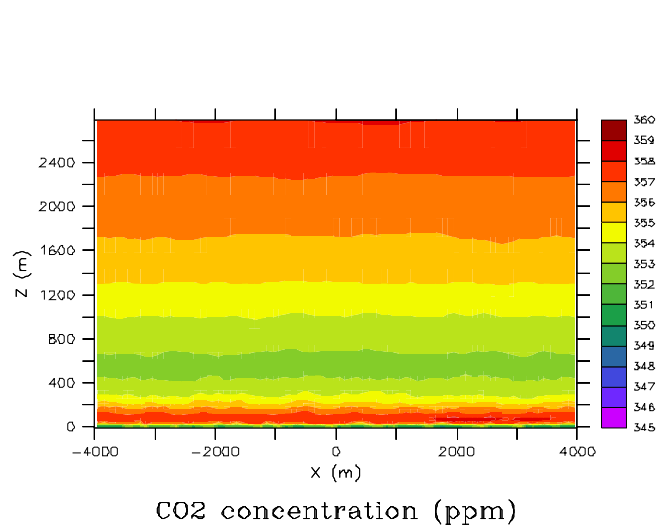


Figure 5: cross-sections of simulated CO₂ concentration in the lower troposphere, simulated by the high-resolution 2-D model. Top-left panel is for 7 AM; Top-right panel is for 9 AM; Bottom-right panel is for 2 PM; Bottom-right panel is for 6 PM.

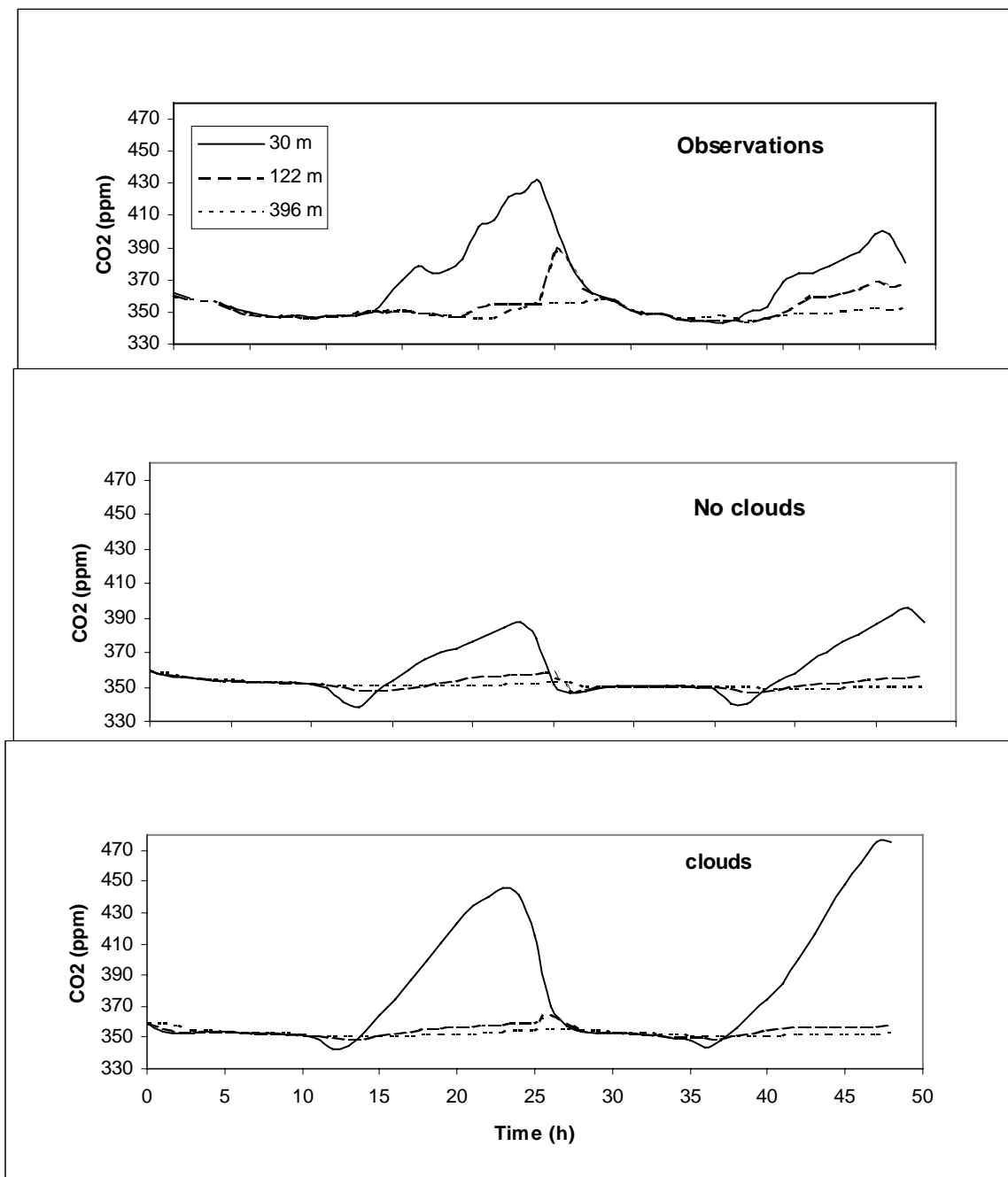


Figure 6: Comparison of simulated and observed CO₂ concentration at three levels on the WLEF-TV tower. Simulations are from the high-resolution 2-D configuration, with and without cloud microphysics.

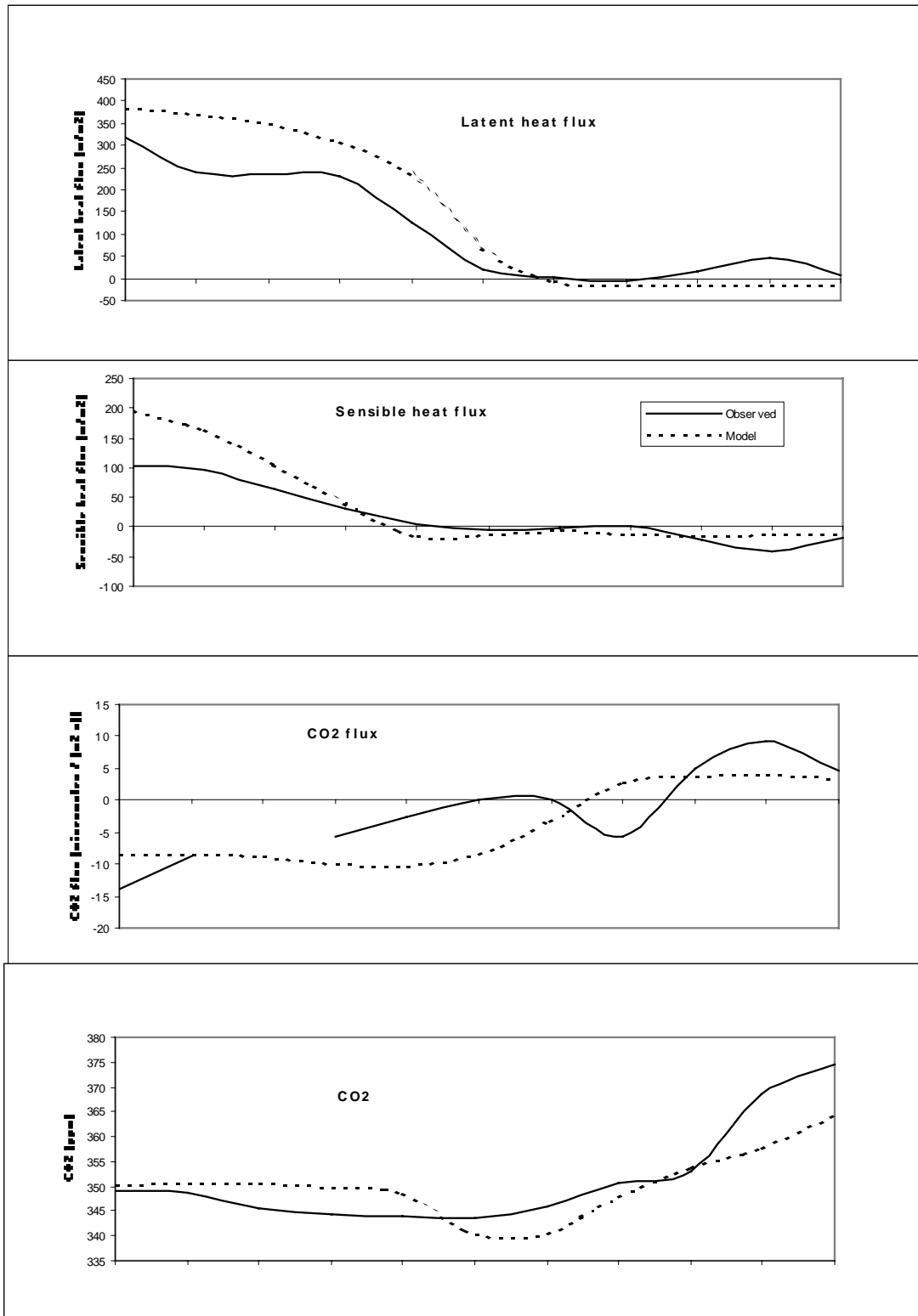


Figure 7: PAR Flux, Rnet, H, LE, NEE in late afternoon, showing the early development of the stable layer in SiB-RAMS which is not observed